Chemical Engineering Journal 151 (2009) 202–208

Contents lists available at ScienceDirect

Chemical Engineering Journal

journal homepage: www.elsevier.com/locate/cej

Theoretical analysis of aggregate densification: Impact on thickener performance

Shane P. Usher*, Rudolf Spehar, Peter J. Scales

Particulate Fluids Processing Centre, Department of Chemical and Biomolecular Engineering, The University of Melbourne, Victoria, 3010, Australia

ARTICLE INFO

Article history:
Received 3 July 2008
Accepted 21 February 2009

Keywords:
Aggregate densification
Gravity thickening
Performance enhancement

ABSTRACT

The aim of gravity thickening processes is to increase the solids concentration of particulate slurries. Gravity thickening depends on the difference in densities between the solid and liquid phases. The solids settle to a more concentrated slurry zone towards the underflow at the thickener base, while relatively solids free liquid rises to the overflow at the top. Predictive modelling of gravity thickener performance from experimentally determined material properties has been shown to under predict throughput by a factor of up to 100. One phenomenon proposed to account for some of this discrepancy is aggregate densification, whereby aggregates compact and become smaller when subjected to shear forces in the thickening process. As the aggregates decrease in size, through densification, the tortuosities around the aggregates will decrease, thus leading to a significant net decrease in the resistance to fluid flow. Dewatering theory has been applied to predict the impact of aggregate densification on the material properties that describe dewatering. The anticipated decrease in aggregate size and associated increase in the density of these aggregates is expected to increase the settling rate. It is further expected on this basis that the material will settle to higher solids concentrations. The impact of these changes on gravity thickening performance is modelled and predicted to be significant.

1. Introduction

Gravity thickening is a critical water recovery and tailings management unit operation in the minerals and other industries. The aim of thickening is to increase the solids concentration of particulate slurries. Gravity thickening depends on the difference in densities between the solid and liquid phases. The solids settle to a more concentrated slurry zone towards the underflow at the thickener base, while relatively solids free liquid rises to the overflow at the top. Materials are usually characterised for thickening through pressure filtration techniques and batch settling tests [1–4]. The properties characterised generally describe the potential extent and rate of dewatering, often quantified as the compressive yield stress, $P_y(\phi)$, and the hindered settling function, $R(\phi)$ [5]. These material properties, $P_y(\phi)$ and $R(\phi)$ can be used in 1D models, and pseudo 2D models accounting for thickener cross-sectional area variations, in order to predict the performance of gravity thickeners [6].

1D thickening performance predictions based on gel point, $R(\phi)$ and $P_y(\phi)$ estimated from batch settling and pressure filtration tests can sometimes underestimate the throughput by a significant factor. It was shown that solids throughput in red mud thickener operations can be up to 100 times higher than predicted [6,7]. With continuous tall column experiments, Gladman [8] showed that the addition of shear in batch settling experiments enhanced the predicted dewatering (and hence the predicted throughput), but the improvement was not sufficient to account for all of the observed discrepancy between laboratory test based predictions and actual thickener performance.

The algorithm used in the thickener predictions described above is limited in that it does not account for material property changes within a thickener as a result of changes in the structure of the material due to shear processes. One phenomenon proposed to account for some of the remaining discrepancy is aggregate densification whereby aggregates compact and become smaller when subjected to shear forces in the thickening process. Polymer flocculation of aggregates is common in thickening processes to improve the sedimentation of particulate slurries. Such shear forces can arise at concentrations less than and above the gel point, from raking processes, sedimentation near and onto thickener walls and floors, buffeting between aggregates, liquid flow around aggregates and also through aggregates. This densification process is postulated to be a relatively irreversible process due to the action of polymer flocculant molecules in holding aggregates together.

The expectation is that when shear is applied, local pressure gradients will be produced resulting in the expulsion of water from the aggregates and subsequent densification. Given the initial

* Corresponding author. Tel.: +61 3 8344 5592; fax: +61 3 8344 4153.
E-mail address: spusher@unimelb.edu.au (S.P. Usher).

1385-8947/$ – see front matter © 2009 Elsevier B.V. All rights reserved.
doi:10.1016/j.cej.2009.02.027

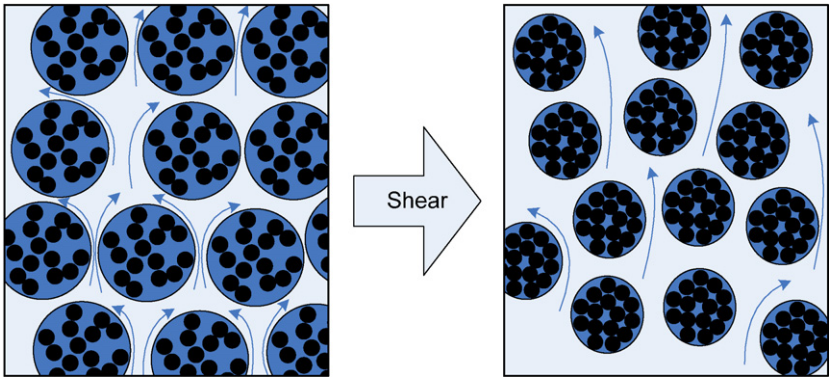

Fig. 1. Effect of aggregate densification on tortuosities between aggregates.

fractal nature of flocculated aggregates produced in a pipe or feedwell [9], this process is likely to result in a more homogeneous, less fractal aggregate [10]. Furthermore, as the aggregates decrease in size, the tortuosities around the aggregates will decrease (i.e. the permeability increases), thus leading to a decrease in the resistance to fluid flow around and an increase in the resistance to fluid flow within the aggregates (see Fig. 1). Thus, it is postulated that by applying shear, additional dewatering occurs before the aggregates reach the bed. However, it has been shown that there is an optimum shear rate beyond which a further increase in the shear rate would be detrimental to aggregate densification, implying a trade off between densification and disintegration of aggregates [8].

Dewatering theory is being applied herein to predict the impact of aggregate densification on the material properties that describe dewatering including the compressive yield stress, $P_y(\phi)$, and hindered settling function, $R(\phi)$. The anticipated decrease in aggregate size and associated increase in the density of these aggregates is expected to increase the settling rate. It is further expected on this basis that the gel point will increase and the compressive yield stress function will reduce for a given solids concentration. Such behaviour is consistent with macroscopic observations of aggregates sampled from a pilot thickener [8]. Mathematical expressions, derived to account for the effect of aggregate densification on the compressive yield stress and hindered settling function have been developed and are presented. These properties are subsequently utilised to predict the theoretical impact of aggregate densification on thickener performance.

2. Theory of aggregate densification

Flocculated aggregates of particles, often referred to as flocs, can be produced by the addition of high molecular weight polymers in the feed well of a thickener. The flocculant forms chemical bridges between particles to create aggregates of much larger diameters than their constituent primary particles. There is always a distribution of primary particle sizes and the aggregates formed also have a distribution of sizes, with variations in aggregate composition and particle density as well.

For the purposes of this analysis, the aggregates will be approximated as roughly spherical in shape, with an average diameter, d_{agg}, quantifying the aggregate size. The overall suspension solids concentration is quantified through the solids volume fraction, ϕ, defined as the total volume of solid particles divided by the total volume of suspension. However, the term ϕ_{agg} is used to quantify the average solids volume fraction within the aggregates. Further, the aggregate volume fraction, φ, is defined as the volume occupied by aggregates divided by the total volume which is logically equal to the overall solids volume fraction, ϕ, divided by the local solids volume fraction within the aggregate, ϕ_{agg}, such that

$$\varphi = \frac{\phi}{\phi_{agg}} \tag{1}$$

A fundamental theory of dewatering was developed by Buscall and White [11]. This theoretical framework forms the basis for experimental methods which quantify the material properties that describe the dewaterability of slurries as a function of solids volume fraction, ϕ. The fundamental material properties employed by the above theory are the gel point, ϕ_g, the compressive yield stress, $P_y(\phi)$, and the hindered settling function, $R(\phi)$. These properties are introduced below with a theoretical analysis of how aggregate densification affects these properties.

2.1. Gel point, ϕ_g, and compressive yield stress function, $P_y(\phi)$, incorporating densification

As isolated aggregates settle to increasingly higher overall solids volume fractions, they will eventually form a spanning network structure at a critical overall solids concentration, known as the gel point, ϕ_g. The solids volume fraction within an aggregate, ϕ_{agg}, is intrinsically linked to this gel point, ϕ_g. For this analysis, the gel point is assumed to be the solids volume fraction at which aggregates form something near to a close packed structure such that,

$$\phi_g = \varphi_p \phi_{agg}, \tag{2}$$

where φ_p is the aggregate packing volume fraction at the gel point. This concept was explored in a previous publication [12]. The aggregate network exhibits a compressive strength, quantified as the compressive yield stress, $P_y(\phi)$, for all solids volume fractions greater than the gel point, ϕ_g.

As aggregate densification occurs, assuming no aggregate breakup, the aggregate diameter, d_{agg}, decreases, causing the solids volume fraction within the aggregates, ϕ_{agg}, to increase. Given that the total amount of solids within an aggregate is constant, irrespective of how much an aggregate diameter might change through densification, a material balance leads to the useful equality,

$$\phi_{agg} d_{agg}^3 = \phi_{agg,0} d_{agg,0}^3, \tag{3}$$

where $\phi_{agg,0}$ and $d_{agg,0}$ are the initial conditions before densification. The variation in ϕ_{agg} as the aggregates densify is given by rearrangement of Eq. (3) such that,

$$\phi_{agg} = \phi_{agg,0} \frac{d_{agg,0}^3}{d_{agg}^3}. \tag{4}$$

Consequently, an increase in ϕ_{agg} during densification causes the gel point, ϕ_g, to increase according to Eq. (2), thereby reducing the

network strength over the range $[\phi_g, \phi_{agg}]$. Incorporating aggregate densification, $P_y(\phi)$, becomes:

$$P_y(\phi) = \left\{ \begin{array}{ll} 0 & : \phi < \phi_g \\ P_{y,1}(\phi) & : \phi_g \le \phi < \phi_{agg} \\ P_{y,0}(\phi) & : \phi_{agg} \le \phi < \phi_{cp} \end{array} \right\}, \quad (5)$$

where $P_{y,0}(\phi)$ represents the undensified compressive yield stress function, initially valid over solids volume fractions ranging from the undensified gel point, $\phi_{g,0}$, to close packing at ϕ_{cp}. $P_{y,1}(\phi)$ is defined over the range (ϕ_g, ϕ_{agg}) such that it is zero at the gel point, ϕ_g, and touches the original undensified compressive yield stress function at the solids volume fraction within the aggregates, i.e.;

$$P_{y,1}(\phi_g) = 0 \quad (6)$$

and

$$P_{y,1}(\phi_{agg}) = P_{y,0}(\phi_{agg}). \quad (7)$$

For the purposes of simplicity in this analysis, it will also be assumed that the gradient $dP_y(\phi)/d\phi$, is single valued at $\phi = \phi_{agg}$, requiring that:

$$P'_{y,1}(\phi_{agg}) = P'_{y,0}(\phi_{agg}) \quad (8)$$

2.2. Hindered settling function, R(ϕ), incorporating densification

The hindered settling function is defined as the hydrodynamic resistance to liquor flow through a solids suspension as a function of solids volume fraction. It is valid for all solids volume fractions as it can be interpreted as either the movement of liquor past a collection of solids or a particle through a liquid. The hindered settling function can also be viewed as being inversely proportional to the permeability of the suspension.

From the fundamental dewatering theory [11], we obtain the following expression for the free settling velocity of particles undergoing sedimentation:

$$u(\phi) = \frac{\Delta\rho.g.(1-\phi)^2}{R(\phi)}, \quad (9)$$

where $\Delta\rho$ is the difference in density between the solid and liquid phases $(\rho_{sol} - \rho_{liq})$ and g is acceleration due to gravity. The magnitude of $R(\phi)$ is related to the hydrodynamic drag coefficient, λ, and the volume of a single particle, V_p, via

$$R(\phi) = \frac{\lambda}{V_p} r(\phi), \quad (10)$$

where $r(\phi)$ is the hindered settling factor which has the following limits:

$$r(\phi) \to 1 \text{ as } \phi \to 0,$$

$$r(\phi) \to \infty \text{ as } \phi \to 1.$$

In this analysis, the settling velocity is assumed to have two contributions; the first from the flow of liquid around aggregates, u_1, and the second from the flow of liquid through aggregates, u_2, such that,

$$u(\phi, d_{agg}) = u_1 + u_2. \quad (11)$$

The flowrate of liquid around the aggregates, u_1, is the dominant contribution to the total settling velocity for unnetworked suspensions at solids concentrations below the gel point, $\phi < \phi_g$. To determine u_1, the aggregates are themselves modelled as 'large sedimenting particles'.

In order to model the effect of aggregate densification within the hindered settling region all aggregates are assumed to be spherical and of equal size. Thus, adapting the settling velocity relation of Eq. (9), to describe the free settling velocity of aggregates, using the concept of an aggregate volume fraction, φ, defined by Eq. (4) gives:

$$u_{agg}(\varphi) = \frac{\Delta\rho_{agg} g (1-\varphi)^2}{\frac{\lambda_{agg}}{V_{agg}} r_{agg}(\varphi)}, \quad (12)$$

where $\Delta\rho_{agg} = \rho_{agg} - \rho_{liq} = \Delta\rho_{agg}$ is the difference in density between the aggregate and liquid phases, λ_{agg} is the hydrodynamic drag on an aggregate, V_{agg} is the volume of an aggregate and $r_{agg}(\varphi)$ is the hindered aggregate settling factor, analogous to the hindered settling function for particles. Note that the aggregate density is given by

$$\rho_{agg} = \phi_{agg}\rho_{sol} + \left(1 - \phi_{agg}\right)\rho_{liq}, \quad (13)$$

such that $\Delta\rho_{agg} = \rho_{agg} - \rho_{liq} = \Delta\rho.\phi_{agg}$. Also, as we have assumed that the aggregates are spherical,

$$\lambda_{agg} = 3\pi\mu d_{agg} \quad (14)$$

and

$$V_{agg} = \frac{\pi d_{agg}^3}{6}. \quad (15)$$

Substitution of Eqs. (13)–(15) into Eq. (12) gives:

$$u_{agg}(\varphi) = \frac{\Delta\rho g}{18\mu} \frac{\phi_{agg} d_{agg}^3}{d_{agg}} \frac{(1-\varphi)^2}{r_{agg}(\varphi)}. \quad (16)$$

Substitution of the material balance in Eq. (3) into Eq. (16) yields the following alternative expression for the liquid flowrate around the aggregates,

$$u_1 = u_{agg}(\varphi) = \frac{\Delta\rho g}{18\mu} \left(\phi_{agg0} d_{agg0}^3\right) \frac{1}{d_{agg}} \frac{(1-\varphi)^2}{r_{agg}(\varphi)}. \quad (17)$$

The velocity contribution due to the flow of liquid through the aggregates, u_2, is given by the settling velocity at the solids volume fraction within the aggregate, $u(\phi_{agg})$, normalised by the aggregate volume fraction, φ, to account for the cross-sectional area of the aggregates relative to the total cross-sectional area, such that,

$$u_2 = \varphi.u(\phi_{agg}) = \varphi.\frac{\Delta\rho.g.\left(1-\phi_{agg}\right)^2}{R(\phi_{agg})}. \quad (18)$$

The potential effect of aggregate densification on the settling velocity and also the effective hindered settling function can now be determined.

Values for the nominal average aggregate size and density are determined, such that these values are consistent with the material properties. The settling velocity of an isolated aggregate, $u(0)$, is determined from the hindered settling function by substitution of $\phi = 0$ in Eq. (9), to give:

$$u(0) = \frac{\Delta\rho.g}{R(0)} \quad (19)$$

Assuming that the liquid flow through the aggregate is negligible relative to the flow of liquid around the particle, Stokes law can be applied for an aggregate, giving:

$$u(0) = \frac{\Delta\rho_{agg}.g.{d_{agg}}^2}{18\mu}, \quad (20)$$

where μ is the liquid viscosity and d_{agg} is the aggregate diameter. Rearranging Eq. (20) gives the following expression for the initial aggregate diameter:

$$d_{agg,0} = \sqrt{\frac{18u(0).\mu}{\Delta\rho_{agg,0}.g}}, \quad (21)$$

Table 1
Variation of $P_y(\phi)$, function parameters (Eq. (25)) with extent of aggregate densification, $d_{agg}/d_{agg,0}$, ranging from 1 to 0.75 given $\phi_{agg,0}=0.1667$, $\varphi_p=0.6$, $\phi_{g,0}=0.1$, $\phi_{cp}=0.8$, $b=0.002$, $a_0=0.9$ and $k_0=11$.

$\frac{d_{agg}}{d_{agg,0}}$	ϕ_{agg}	ϕ_g	a_1	k_1
1.00	0.1667	0.1000	0.9000	11.000
0.95	0.1944	0.1166	0.8677	10.428
0.90	0.2286	0.1372	0.8594	10.363
0.85	0.2714	0.1628	0.8615	10.469
0.80	0.3255	0.1953	0.8676	10.618
0.75	0.3951	0.2370	0.8747	10.757

A consistent hindered aggregate settling factor, $r_{agg}(\varphi)$ is determined by rearranging the terms in $u(\phi,d_{agg,0})=u(\phi)=u_1+u_2$ from Eqs. (9), (17) and (18) to give:

$$r_{agg}(\varphi)=\frac{\Delta\rho.g}{18\mu}\frac{\phi_{agg0}d_{agg0}^3}{d_{agg}}\frac{(1-\varphi)^2}{\left(u(\phi)-\varphi.u(\phi_{agg})\right)}, \tag{22}$$

which is valid for all aggregate volume fractions from 0 to 1.

The effective hindered settling function subject to aggregate densification, $R(\phi,d_{agg})$, is determined from a rearrangement of Eq. (9) to give:

$$R(\phi,d_{agg})=\frac{\Delta\rho.g.(1-\phi)^2}{u(\phi,d_{agg})}, \tag{23}$$

such that $u(\phi,d_{agg})$ is determined using Eqs. (17) and (18).

3. Model densification case study

Functional forms and parameter values for undensified $P_y(\phi)$ and $R(\phi)$ properties have been chosen such that they are representative of flocculated industrial slurries produced in the feedwells of large scale gravity thickeners. Six cases are presented, representing a range of aggregate densification extents varying from the original undensified structure with diameter $d_{agg,0}$ to aggregates that have densified to 75% of their original diameter, $0.75\,d_{agg,0}$. Application of the densification theory above, in a model case study, demonstrates how $P_y(\phi)$ and $R(\phi)$ are predicted to change when the aggregates densify. Further, these modified properties are used to predict the impact of aggregate densification on steady state thickener performance.

3.1. Network strength

Using the assumed initial values, $\phi_{g,0}=0.1$ and $\varphi_p=0.6$, Eq. (2) enables determination of the initial solids volume fraction within the aggregate, $\phi_{agg,0}=0.1667$. In this model case study, the undensified compressive yield stress function, $P_{y,0}(\phi)$, which is greater than zero for all solids volume fractions greater than the undensified gel point, $\phi_{g,0}$, up to a close packing solids volume fraction, ϕ_{cp} (assumed = 0.8 in this analysis), is given by

$$P_{y,0}(\phi)=\left(\frac{a_0(\phi_{cp}-\phi)(b+\phi-\phi_{g,0})}{(\phi-\phi_{g,0})}\right)^{-k_0}, \tag{24}$$

where the function parameters a_0, k_0 and b have assumed values of 0.9, 11 and 0.002, respectively. Incorporating aggregate densification, the $P_{y,1}(\phi)$ function described in Eq. (5) becomes:

$$P_{y,1}(\phi)=\left(\frac{a_1(\phi_{cp}-\phi)(b+\phi-\phi_g)}{(\phi-\phi_g)}\right)^{-k_1} \tag{25}$$

where a_1 and k_1 are determined such that the gradient $dP_y(\phi)/d\phi$, is smooth and continuous at $\phi=\phi_{agg}$, giving:

$$k_1=\left(\frac{P'_{y,0}(\phi_{agg})}{P_{y,0}(\phi_{agg})}\right)\frac{\left(\phi_{cp}-\phi_{agg}\right)\left(\phi_{agg}-\phi_g\right)\left(b+\phi_{agg}-\phi_g\right)}{b\left(\phi_{cp}-\phi_g\right)+\left(\phi_{agg}-\phi_g\right)^2} \tag{26}$$

and

$$a_1=\frac{\left(P_{y,0}(\phi_{agg})\right)^{-1/k_1}\left(\phi_{agg}-\phi_g\right)}{\left(\phi_{cp}-\phi_{agg}\right)\left(b+\phi_{agg}-\phi_g\right)}, \tag{27}$$

where from Eq. (24),

$$P_{y,0}(\phi_{agg})=\left(\frac{a_0(\phi_{cp}-\phi_{agg})(b+\phi_{agg}-\phi_{g,0})}{(\phi_{agg}-\phi_{g,0})}\right)^{-k_0} \tag{28}$$

and the gradient $P'_{y,0}(\phi_{agg})$ is calculated to be:

$$P'_{y,0}(\phi_{agg})=-a_0k_0\frac{\left(\frac{(\phi_{cp}-\phi_{g,0})}{(\phi_{agg}-\phi_{g,0})}-1-\frac{(\phi_{cp}-\phi_{g,0})(b+\phi_{agg}-\phi_{g,0})}{(\phi_{agg}-\phi_g)^2}\right)}{\left(a_0\left(b+\phi_{agg}-\phi_{g,0}\right)\left(\frac{(\phi_{cp}-\phi_{g,0})}{(\phi_{agg}-\phi_{g,0})}-1\right)\right)^{k_0+1}} \tag{29}$$

As aggregate densification occurs, the aggregate diameter, d_{agg}, decreases and according to Eqs. (2) and (4), ϕ_{agg} and ϕ_g, are predicted to increase, as shown in Table 1, demonstrating the significant increase in aggregate densification that can be obtained, from only a minor change in aggregate diameter. The corresponding values of a_1 and k_1, determined using Eqs. (26)–(29), are also shown in Table 1. Given the parameters listed in Table 1, the compressive yield stress function has been graphed, in Fig. 2, for aggregate densification extents ranging from the original aggregate diameter, $d_{agg,0}$, to $d_{agg}/d_{agg,0}=0.75$. This data is similar in form to experimental data measured by Gladman [8] for sheared sedimentation of aggregates.

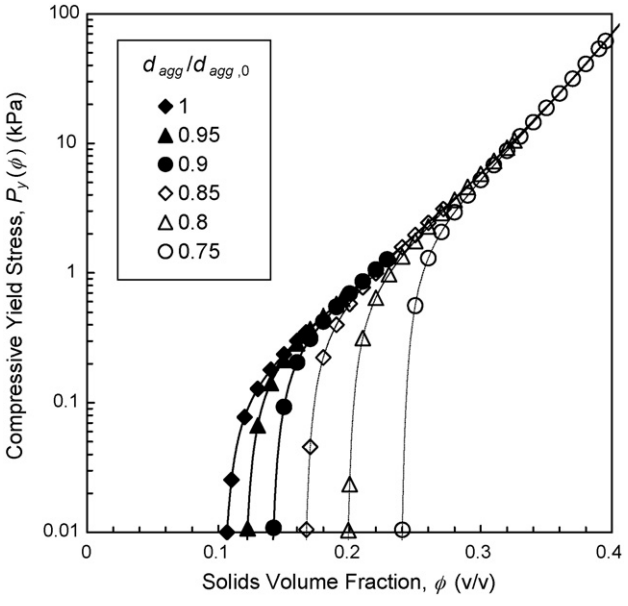

Fig. 2. Example of compressive yield stress function, $P_y(\phi)$, curves using the functional form given by Eq. (5), (24) and (25) and parameter values given in Table 1 for a range of aggregate densification extents ranging from the original aggregate diameter, $d_{agg,0}$, to $d_{agg}/d_{agg,0}=0.75$.

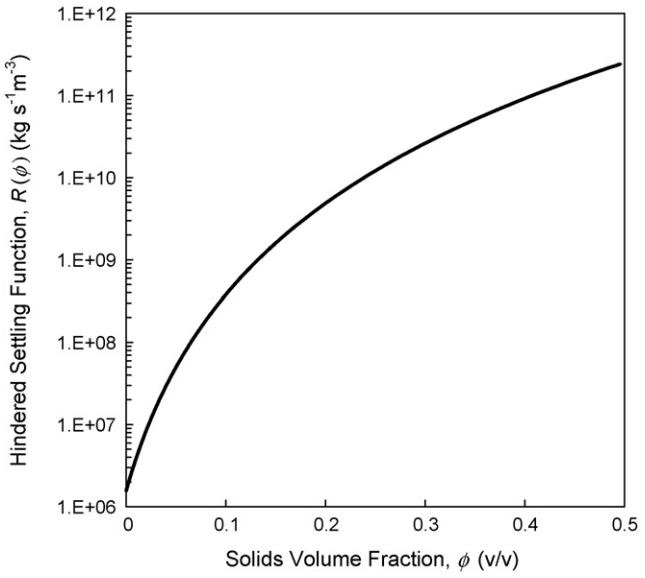

Fig. 3. Example of hindered settling function, $R(\phi)$, curve fit using the functional form given by Eq. (30) with parameter values $r_a = 5 \times 10^{12}$, $r_b = 0$, $r_g = -0.05$ and $r_n = 5$.

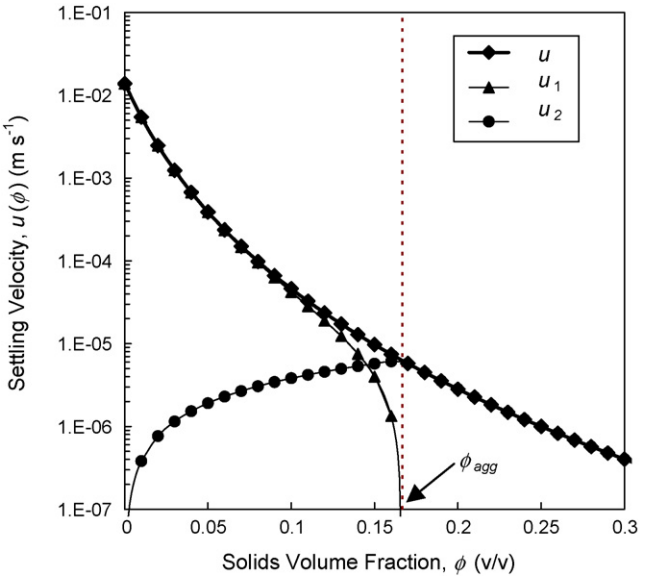

Fig. 5. Variation of suspension settling velocities with solids volume fraction, where u is the total settling velocity, u_1 is the velocity component which flows around the aggregates and u_2 is the velocity component which flows through the aggregates.

3.2. Rate of dewatering

A model hindered settling function equation is given by

$$R(\phi) = r_a\left(\phi - r_g\right)^{r_n} + r_b, \tag{30}$$

where r_a, r_b, r_g and r_n are empirical fitting parameters. A curve using parameter values representative of a flocculated mineral tailings slurry is shown in Fig. 3.

Using the $R(\phi)$ parameter values ($r_a = 5 \times 10^{12}$, $r_b = 0$, $r_g = -0.05$ and $r_n = 5$), the hindered settling function of an isolated aggregate is calculated to be, $R(0) = 1.5625\text{e+}06\ \text{kg s}^{-1}\ \text{m}^{-3}$. Given typical values for the solids density, $\rho_{sol} = 3200\ \text{kg m}^{-3}$ and the liquid density, $\rho_{liq} = 1000\ \text{kg m}^{-3}$, $\Delta\rho = 2200\ \text{kg m}^{-3}$ and $g = 9.8\ \text{m s}^{-2}$ in Eq. (19), the undensified isolated aggregate settling velocity is calculated to be, $u(0) = 0.013798\ \text{m s}^{-1}$. Given the initial solids volume fraction within the aggregate, $\phi_{agg,0} = 0.1667$, the initial aggregate density, $\rho_{agg,0} = 1366.7\ \text{kg m}^{-3}$ is calculated from Eq. (13), to give the initial aggregate to liquid density difference, $\Delta\rho_{agg,0} = 366.7\ \text{kg m}^{-3}$. Using Eq. (21) with the liquid viscosity, $\mu = 0.001$ Pa s, the initial aggregate diameter, $d_{agg,0}$ is calculated to be 262.9 μm.

As the solids volume fraction within an aggregate increases, the gravitational impetus for settling would improve because the density difference between the aggregate and liquid increases significantly, as shown in Fig. 4. The total, internal and external flow velocity contributions, determined from Eq. (9) for u, Eq. (18) for u_2 and by difference for u_1 are shown in Fig. 5, demonstrating that flow through the aggregates is only expected to be significant relative to the flow around the aggregates as the solids volume fraction approaches and exceeds that inside the aggregates. The calculated hindered aggregate settling factor, $r_{agg}(\varphi)$, determined using Eq. (22) and shown in Fig. 6, is assumed to be generic and not subject to change as aggregates densify. Note that $r_{agg}(\varphi)$ is not defined when

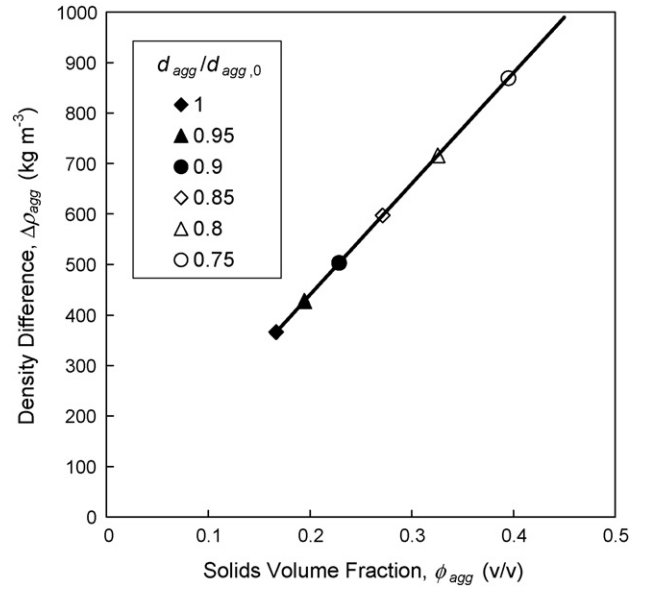

Fig. 4. Variation of aggregate-liquid density difference with aggregate solids volume fraction.

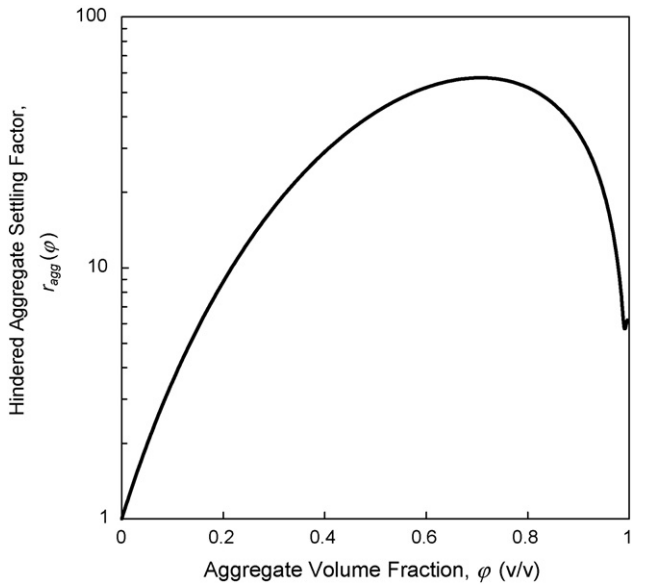

Fig. 6. Variation of hindered aggregate settling factor with aggregate volume fraction, derived from hindered settling function and aggregate solids volume fraction.

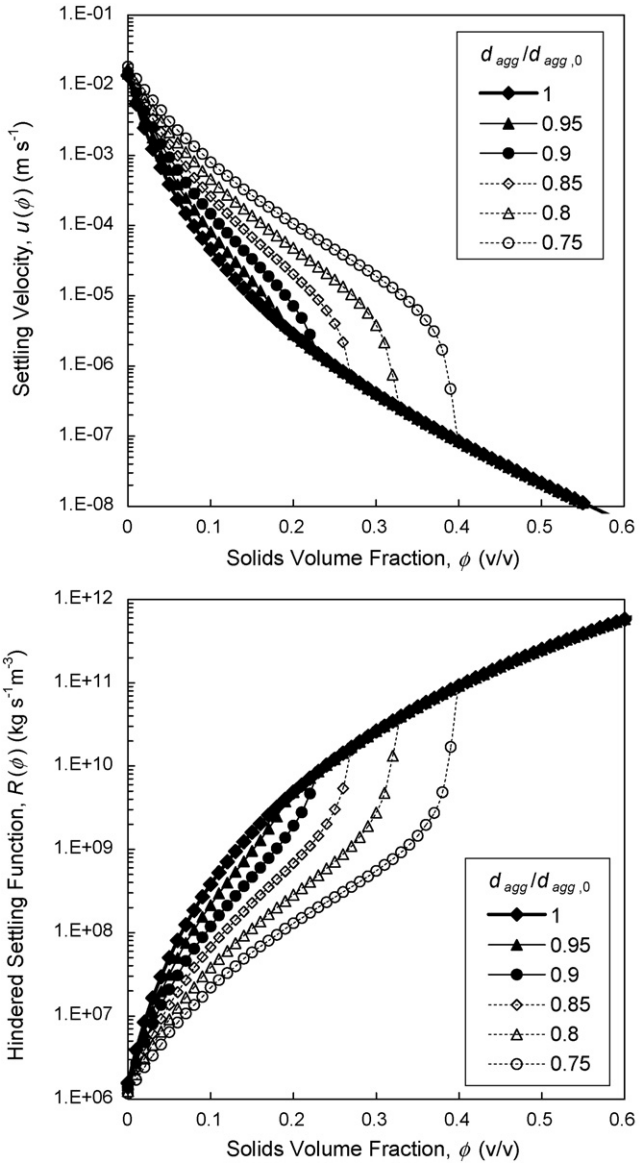

Fig. 7. Variation of overall settling velocity and hindered settling function versus solids volume fraction for a range of aggregate densification extents ranging from the original aggregate diameter, $d_{agg,0}$, to $d_{agg}/d_{agg,0} = 0.75$.

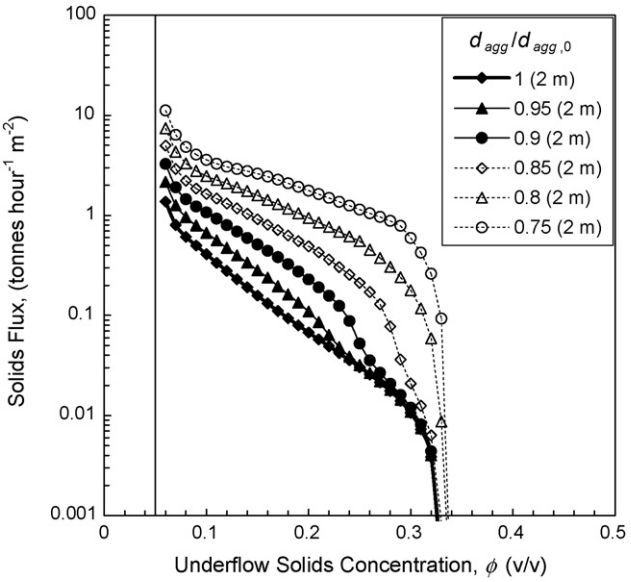

Fig. 8. Steady state thickener performance predictions in terms of solids flux versus solids volume fraction, ϕ, for a range of aggregate densification extents ranging from the original aggregate diameter, $d_{agg,0}$, to $d_{agg}/d_{agg,0} = 0.75$.

$\varphi > 1$, or alternatively $\phi > \phi_{agg}$, because conceptually the aggregates are fully networked with no gaps, such that $u_1 = 0$ and only flow through the aggregates is relevant. The validity of the Stokes law behaviour assumption, for Eq. (12), relies on the Reynolds number being low. In the modelling presented, the maximum Reynolds number, $Re \approx 8$ at $\phi = 0$, reducing to $Re \ll 1$ as ϕ increases. Though Stokes Law loses accuracy for $Re > 1$, this loss of accuracy is not expected to significantly affect the effective permeability enhancement predicted in this analysis.

The variation of the total settling velocities, $u(\phi,d_{agg})$, versus solids volume fraction for a range of aggregate densification extents is shown in Fig. 7, demonstrating the significant potential for improvement in settling velocity from aggregate densification. Fig. 7 shows the variation of the effective hindered settling function subject to aggregate densification, $R(\phi,d_{agg})$, determined from Eq. (23). For solids volume fractions up to the aggregate volume fraction, significant reductions in the hindered settling function are predicted. For higher solids volume fractions, no additional improvement is predicted.

The improvement in permeability is predicted to increase significantly with aggregate densification, such that when $d_{agg}/d_{agg,0} = 0.75$, the maximum predicted improvement is a factor of 48. For each aggregate diameter, the maximum predicted improvement occurs when φ is in the range 0.6–0.75. When $\varphi > 1$, no improvement in the permeability is predicted. However, it is of interest to discuss what φ physically represents when the slurry becomes networked. A simple interpretation is that at solids concentrations above the gel point, it is the interstices between the aggregates that are eliminated first, before subsequent compression of the cake occurs. In this way, the suspension structure will become more homogeneous as the solids concentration increases until the structure is independent of its formation conditions. Though not predicted by this analysis, permeability improvement could also occur at high solids concentrations, $\varphi > 1$ or $\phi > \phi_{agg}$, but theoretical prediction of this behaviour would be difficult.

4. Thickener performance: theoretical prediction

The dewatering material properties, $P_y(\phi)$ and $R(\phi)$, described above for a range of aggregate densification extents, have been used as inputs in steady state thickener performance predictions for a straight sided thickener using an algorithm described by Usher and Scales [6]. These thickener performance predictions, in terms of solids flux versus underflow solids volume fraction are shown in Fig. 8 for operation with a feed solids volume fraction of 0.05 and 2 m of bed height. These predictions demonstrate significant potential for aggregate densification to improve both the rate and extent of dewatering in thickener operation.

Performance enhancement factors, *PE* = *solids flux* (*densified*)/*solids flux* (*original*), have been calculated and are shown in Fig. 9 as functions of solids volume fraction for a range of aggregate densification extents. The performance enhancement is predicted to increase significantly with aggregate densification. At high solids fluxes and low underflow solids concentrations, the magnitude of the *PE* is dominated by the improvement in permeability quantified by the hindered settling function, $R(\phi)$. However, at low solids fluxes and high underflow solids concentrations, changes in $P_y(\phi)$ also influence performance, increasing the maximum possible underflow solids volume fraction with the extent of densification.

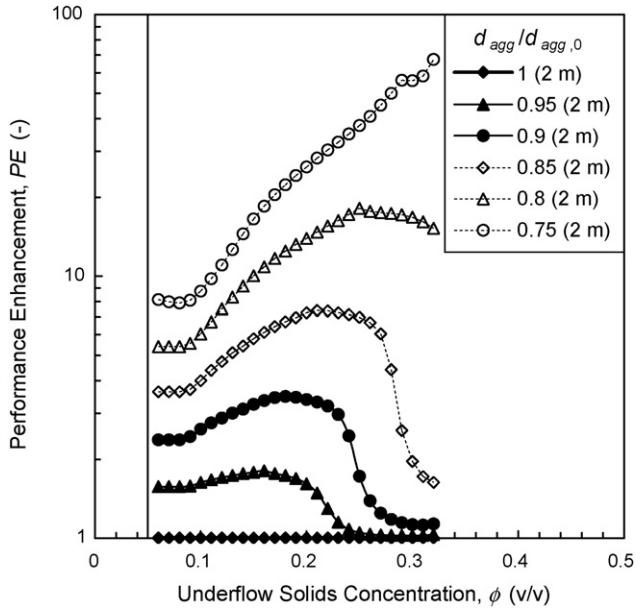

Fig. 9. Performance enhancement factor, *PE*, versus solids volume fraction, ϕ, for a range of aggregate densification extents ranging from the original aggregate diameter, $d_{agg,0}$, to $d_{agg}/d_{agg,0} = 0.75$.

The peak in the performance enhancement graph for small extents of densification could be used as a guide to indicate the optimum extent of dewatering for a given extent of densification in a thickener.

Experimental observations of aggregate densification can be obtained from raked settling tests and also from fluidisation tests [8], providing knowledge of the residence time and shear rate history dependence. It is expected that the combination of such experimental data and this aggregate densification theory will be used to predict how the rate at which aggregates densify within a thickener, as the solids concentration increases. Subsequently, there is potential for geometric factors such as cross-sectional area variation and shear processes to be optimised to maximise performance enhancement throughout the thickening process. It is currently an open question as to the significance of aggregate densification in causing improved dewatering in practice. However, observations from laboratory and fieldwork are consistent with the densification hypothesis described herein. Even if densification is not the overwhelmingly dominant contributor, it would seem to be highly desirable to develop thickening techniques that cause densification phenomena to be optimised.

5. Conclusions

Dewatering theory has been developed to include the effect of aggregate densification on material properties that describe the rate and extent of dewatering. It has been demonstrated that aggregate densification enables increased sedimentation velocity to higher solids concentrations and would account for some of the performance enhancement observed in thickening processes. Depending on the solids concentration and extent of densification, performance improvements by up to a factor of 50 are predicted.

Acknowledgements

This work was conducted as part of AMIRA P266E: Improving Thickener Technology and supported by the Australian Research Council (ARC) under the Linkage Scheme.

The authors also acknowledge the support of the PFPC (Particulate Fluids Processing Centre), a Special Research Centre of the ARC.

References

[1] D.R. Lester, S.P. Usher, P.J. Scales, Estimation of the hindered settling function $R(\phi)$ from batch-settling tests, AIChE J. 51 (4) (2005) 1158–1168.
[2] S.P. Usher, R.G. de Kretser, P.J. Scales, Validation of a new filtration technique for dewaterability characterization, AIChE J. 47 (7) (2001) 1561–1570.
[3] G.J. Kynch, A theory of sedimentation, Trans. Faraday Soc. 48 (1952) 166–176.
[4] R.G. de Kretser, S.P. Usher, P.J. Scales, D.V. Boger, K.A. Landman, Rapid filtration measurement of dewatering design and optimization parameters, AIChE J. 47 (8) (2001) 1758–1769.
[5] K.A. Landman, L.R. White, Solid/liquid separation of flocculated suspensions, Adv. Colloid Interface Sci. 51 (1994) 175–246.
[6] S.P. Usher, P.J. Scales, Steady state thickener modelling from the compressive yield stress and hindered settling function, Chemical Engineering Journal 111 (2–3) (2005) 253–261.
[7] S.P. Usher, Suspension dewatering: characterisation and optimisation, in Particulate Fluids Processing Centre, in: Department of Chemical Engineering, The University of Melbourne, Melbourne, Australia, 2002, p. 347.
[8] B.R. Gladman, The effect of shear on dewatering of flocculated suspensions, in: Department of Chemical and Biomolecular Engineering, The University of Melbourne, Melbourne, Australia, 2004, p. 332.
[9] A.R. Heath, P.A. Bahri, P.D. Fawell, J.B. Farrow, Polymer flocculation of calcite: relating the aggregate size to the settling rate, AIChE J. 52 (6) (2006) 1987–1994.
[10] G.C. Bushell, Y.D. Yan, D. Woodfield, J. Raperc, R. Amala, On techniques for the measurement of the mass fractal dimension of aggregates, Adv. Colloid Interface Sci. 95 (2002) 1–50.
[11] R. Buscall, L.R. White, The consolidation of concentrated suspensions, J. Chem. Soc. Faraday Trans. I 83 (1987) 873–891.
[12] S.P. Usher, Y. Zhou, G.V. Franks, P. Scales, Determination of the gel point from the fractal dimension, in: Proceedings of CHEMECA 2007, Engineers Australia, Melbourne, Australia, 2007.